

Contribution of Metasilicates Containing TENORM to Radon Activity Concentration in Building Materials

Antonella Nicolino

ARPACAL, Ettore Majorana Physics Laboratory

Mattia Rocco Ligato

ARPACAL, Ettore Majorana Physics Laboratory

Mario Ferraro (✉ mario.ferraro@uniroma1.it)

Sapienza University of Rome <https://orcid.org/0000-0002-6014-2890>

Salvatore Procopio

ARPACAL, Ettore Majorana Physics Laboratory

Research Article

Keywords: Radon activity, NORM and TENORM, Phosphorites, Indoor exposure, Crotona, Building materials

Posted Date: June 14th, 2021

DOI: <https://doi.org/10.21203/rs.3.rs-530939/v1>

License:  This work is licensed under a Creative Commons Attribution 4.0 International License.

[Read Full License](#)

Contribution of metasilicates containing TENORM to radon activity concentration in building materials

Antonella Nicolino⁽¹⁾, Mattia Rocco Ligato⁽¹⁾, Mario Ferraro^(2,*) and Salvatore Procopio^(1,**)

⁽¹⁾ ARPACAL, Ettore Majorana Physics Laboratory -Department of Catanzaro,
Via Lungomare, 88100 Catanzaro, Italy

⁽²⁾ Department of Information Engineering, Electronics and Telecommunications (DIET),
Sapienza University of Rome, Via Eudossiana 18, 00184 Rome, Italy

* mario.ferraro@uniroma1.it;

** s.procopio@arpacal.it

Abstract

Radon exhalation from soil and ores is among the most dangerous risks for the public health care. The impact becomes even more powerful when technological enhanced naturally occurring radioactive materials (TENORM) are used for public and private building. Here, we report the realization of a down-scaled model of a building, whose construction materials contain TENORM harvested in a site in Crotone (Italy). We observe an increase of the radon activity in the model when TENORM residues are employed. These results have then been compared to a real use case. The correspondence found between the values of radon activity concentration in the model and in the use case suggests that estimating the radon concentration is an useful method to target TENORM presence inside buildings.

Keywords: Radon activity, NORM and TENORM, Phosphorites, Indoor exposure, Crotone, Building materials

1 - Introduction

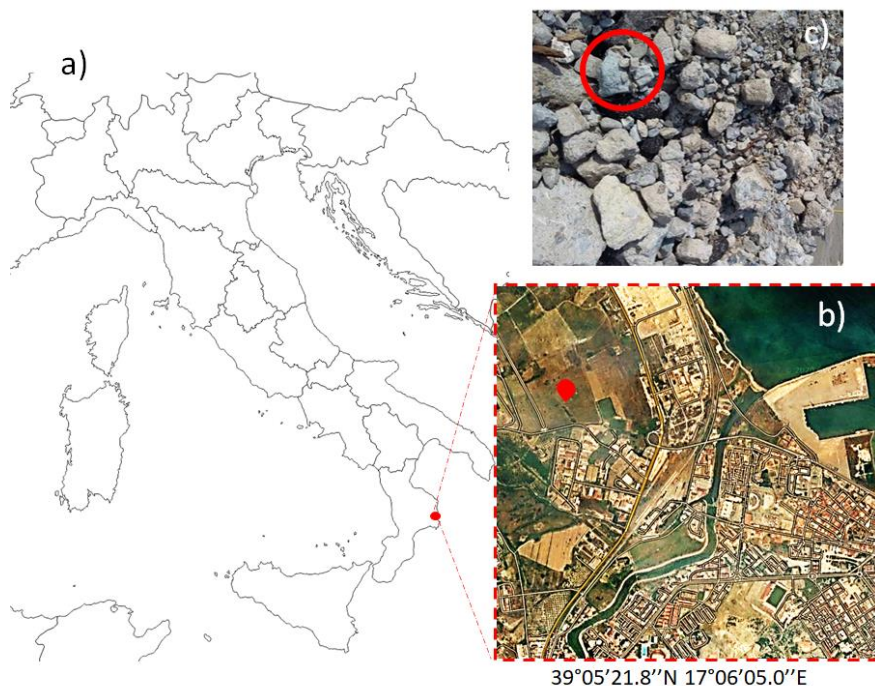
Radon is an inert natural gas whose detection finds application in several fields from geology (Noguchi 1977; Fleischer 1978; Dimova 2011) to public health care (Rutherford 1995) and (although controversially) in astrophysics (Pommé 2019). All these applications exploit the activity of the Radon-222 isotope (^{222}Rn) that belongs to the Uranium-238 (^{238}U) decay chain and has an half-life time of about 3.8 days. For this reason, ^{222}Rn is radioactive and therefore it is dangerous: ^{222}Rn activity has been shown to provide damages to health, attracting a worldwide interest of the scientific community (Lysandrou 2007; Yanchao 2020). A particular focus has been given by the European Commission to radon in the directive 59/2013 that reinforces the regulation about the population exposition to radioactivity (Euratom 2013).

The ^{222}Rn activity can be easily monitored in uranium mines, where the concentration may become remarkably high (Sahu 2013). Nevertheless, in the last decades, many studies have been carried out to estimate the impact of the ^{222}Rn exhalation over the ground from soil (Bossey 2003), building materials (Zhang 2012; Keller 2001) and NORM (Tufail 2010; Dentoni 2020), acronyms of Naturally Occurring Radioactive Materials. Among the latter, particularly interesting is the case of phosphorite rocks that are rich of ^{238}U and Thorium-232 (^{232}Th) (Menzel 1968). Their extraction and processing were the base for producing phosphoric acid, finding application in fertilizers, detergents, feeds, food additives and pesticides (Silva 2006; El Afifi 2009).

50 Processing NORM may results in the production of TENORM (Technological Enhanced Naturally
51 Occurring Radioactive Materials) residues that, in the case of phosphorite rocks, contain naturally
52 radioactive phosphogypsum and metasilicates (Nero 1984; Stoulos 2003).
53 Remarkable is the case of Crotone that since 1928 until the beginning of 1990 was one of the most
54 important chemical industrial city in Europe, specialized in the treatment of phosphorite rocks,
55 imported from Algeria and Morocco. For this reason, nowadays Crotone hosts in its territory
56 residues of processed materials containing TENORM, enhancing the environmental radioactive
57 level (Caridi 2017). Furthermore, over the years, because of their useful mechanical properties,
58 these residues were used in the construction of public and private roads as well as closed spaces,
59 such as dwellings, warehouses and public buildings. Thus, an important mass of phosphoric
60 metasilicate is dangerously present all over the city, possibly determining an increase in the
61 effective radiation dose for the population (Santagati 2016; Andresz 2019).
62 In this work, we propose a way to estimate the presence of TENORM in building by monitoring the
63 indoor ^{222}Rn concentration. For this purpose, we built an in-scale model of a house including
64 phosphorite residues harvested in the city as building materials. The effect of such residues on the
65 environmental radioactivity has been monitored by means of both active and passive devices. We
66 found a significant increase of the ^{222}Rn activity concentration inside the house model. The
67 experimental values obtained in the model are compared to a real use case, i.e. an industrial
68 warehouse where the employment of TENORM had been previously checked. A rather good
69 agreement is found, indicating that ^{222}Rn can be used as a TENORM precursor to indirectly
70 determine and to map the phosphorite contamination.

71 72 2 - Materials

73
74 The materials used in our experiments are phosphorite residues coming from a site targeted as a
75 potential radioactive pole in Crotone: a square in front of a former high school (named Ciapi, whose
76 exact location is reported in Fig.1a,b). Despite the amount of residues originally present in the city
77 is unknown, a rough estimation of thousands of tons can be done by seeking the factories
78 production history (Santagati 2016). Phosphorite TENORM are easily recognizable by their unique
79 blue color (see the picture in Fig.1c).

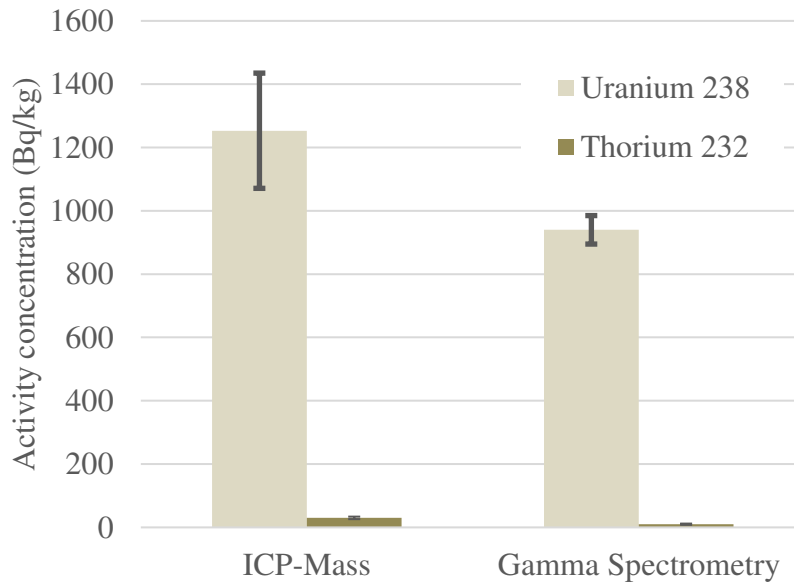


80
81 *Figure 1: a) Crotone position in the Italian map. b) Harvesting site location. c) Picture of the*
82 *phosphorite rocks showing their typical blue colour.*
83

84 Tracing their historical origin, we found that such residues come from the industrial zone where
 85 mainly two chemical processes used to be developed: the extraction of phosphorus from sulphuric
 86 acid and the thermal production of elemental phosphorus. The first results in the production of
 87 phosphogypsum that, due to its flour-like nature, was not useful as construction material.
 88 Conversely, the second exploits a thermal reaction in blast furnaces between phosphorite and silica
 89 (SiO_2) using either iron or carbon (C) as catalysers (Erkens 1999):



92
 93 The silica main role consists of extracting the calcium (Ca) from the calcium phosphate
 94 ($\text{Ca}_3(\text{PO}_4)_2$). At the same time, this insulates the elemental phosphorus giving a glassy nature to the
 95 metasilicates (CaSiO_3). These are the only solid residues of the reaction, since both the carbon
 96 oxide (CO) and elemental phosphorus (P_4) are gases. Reaction (1) is only one of the chemical
 97 process that take place during the thermal production of elemental phosphorus. Indeed,
 98 phosphorites are complex minerals, constituted of many chemical elements that are involved in the
 99 reaction (e.g., aluminium and lead) (Tayibi 2009). Among them, despite some naturally radioactive
 100 elements like the Polonium-210 are ejected during the process, other elements, such as ^{232}Th , ^{238}U ,
 101 Radium-226 and some of lead isotopes, are possibly accumulated inside the metasilicates. This
 102 provides a natural radioactivity to the residues that are therefore labelled as TENORM (El Afifi
 103 2006). As a first step of our study, we characterized the radiometric features of the residues, having
 104 a density $\rho = 1220 \text{ kg/m}^3$. In Fig.2 we report the activity concentration of ^{238}U and ^{232}Th , measured
 105 both by ICP-Mass and γ -spectrometry. The results given by the two techniques are compatible: the
 106 ^{238}U contribution is about 1000 Bq/kg while that of ^{232}Th is two order of magnitude smaller.
 107 Coherently, one can expect an appreciable ^{222}Rn activity. Once characterized, these rocks were
 108 employed in the model building, as it will be discussed below.
 109
 110



111

	Activity concentration [Bq/kg]	
	ICP-Mass	γ -spectrometry
^{238}U	1253±182	940±45
^{232}Th	30±4	10±2

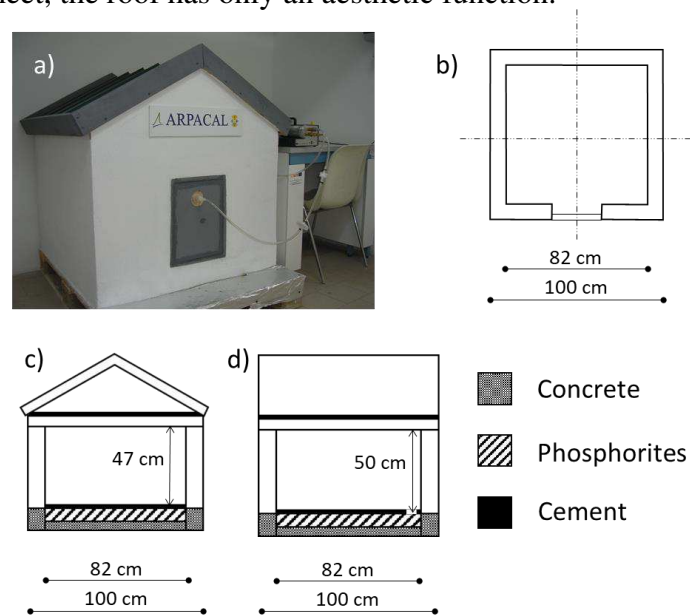
112

113

Figure 2: Uranium and Thorium activity concentration measured by ICP-Mass and γ -spectrometry.

114 **3 - Model**

115 Our model is a down-sized reproduction of a typical city dwelling, shown in Fig.3a. The house,
116 having a 1.00 m x 1.00 m square area, was named Mary's House, being Mary the most popular
117 name in the city. In Fig.3b, we show the model planimetry. A door, properly sealed during the
118 measurements, was added to the square perimeter in order to access the inside volume where the
119 experiments are carried out. Significant accuracy was spent on details such as the thickness of the
120 walls, the relative air chamber, the interior and the exterior plasters. In particular, the wall thickness
121 is about 10 cm in the foundations and 9 cm in the house so that the accessible area is 82 cm x 82
122 cm. The inside space is about 50 cm high without considering the roof and the foundation volumes,
123 as depicted in Fig.3c. The figure also details the different materials employed. After interviewing
124 building workers, we replicated the techniques used in the '80s and '90s in order to obtain a re-
125 production as faithful as possible. According to these techniques, the residues were systematically
126 used as an inert material for filling buildings crawlspaces and foundations. For sake of simplicity, in
127 our model we employ phosphorite residues only to fill the crawlspace, being 7 cm deep. In this
128 way, we could have a better estimation of the background activity as described in the following
129 sections. Filling the crawlspace required a mass of (61 ± 1) kg, on top of which a 3 cm thick screed
130 of cement mortar has been made (see the different heights reported in Fig.3c and 3d). Conversely,
131 we made the foundation of reinforced concrete (with a specific weight of 23.5 kN/m^3) on a raft of
132 the same material. The curtain walls are made of forated bricks (with a specific weight of 8 kN/m^3),
133 vertically arranged in order to increase the volume of the air present inside the walls, whereas the
134 roof slab is constituted of a flooring blocksand and a cement mortar screed. After plastering, the
135 whole house was painted both internally and externally with washable paint. The plaster has been
136 made as thin as possible in order to avoid possible ^{222}Rn absorption. Finally, consisting of two
137 layers of corrugated sheet, the roof has only an aesthetic function.



138
139

140 *Figure 3: Building Details of Mary's House. a) Picture of the in-scale house model; b) Planimetry*
141 *of the house; c-d) Model sections along the two dashed lines in b) with building material details.*

142
143

143 **4 - Methods**

144
145

145 The ^{222}Rn activity was measured by means of both active and passive devices. In particular, for a
146 real-time monitoring, we used a Lucas cell device (one may noting it connected to the door in the
147 picture of Fig.3a). This allows us to simultaneously monitor the ^{222}Rn activity and the
148 environmental parameters such as the temperature, the pressure and the humidity. On the other
149 hand, passive devices, such as CR39s and electrets, provide long time and more accurate activity

150 concentration estimation. The electret-based method involves electrostatic measurements so that the
151 ^{222}Rn activity concentration $[\text{}^{222}\text{Rn}]$ can be obtained as (Caresana 2005)

152
153
$$[\text{}^{222}\text{Rn}] = \left(\frac{V_i - V_f}{C_f \cdot t_e} - C_\gamma \right) \cdot H \quad (2)$$

154
155 where V_i and V_f are the initial and final surface potential respectively, C_f is a calibration coefficient,
156 C_γ is the γ -radiation equivalent ^{222}Rn concentration, H is a factor taking into account the altitude,
157 and t_e is the exposition time. The parameter C_γ is measured by putting an electret, dubbed
158 “witness”, in an hermetic closed plastic bag in order to evaluate the electrostatic potential drop due
159 to γ -radiation. On the other hand, the CR39-based method consists of counting the traces formed on
160 a plastic material by α particles emitted during the ^{222}Rn decay. These are directly proportional to
161 the activity concentration (Kropat 2015)

162
$$[\text{}^{222}\text{Rn}] = \frac{\rho_{\text{net}} \cdot k}{t_e} \quad (3)$$

163
164 where ρ_{net} is the density of clear traces in the detector sensitive area (in our case 25 mm x 25 mm)
165 and k is an instrumental calibration factor. In order to enlarge the traces and make them visible at
166 the microscope, the CR39s were soaked for one hour in a sodium hydroxide (6.25 molar) bath at
167 98°C. The number of traces was then recorded by an automatic optical reader (Politrack microscope
168 from Miam srl). In Fig.4 we report pictures of the microscope and the detectors used in the
169 experiments. When using passive devices, we kept tracking the ^{222}Rn concentration as well as the
170 pressure, humidity and temperature by the Lucas cell. In this way, the experimental condition
171 stability was ongoingly monitored. Significant variations of these parameters were never observed
172 during all the experimental campaigns.

173
174

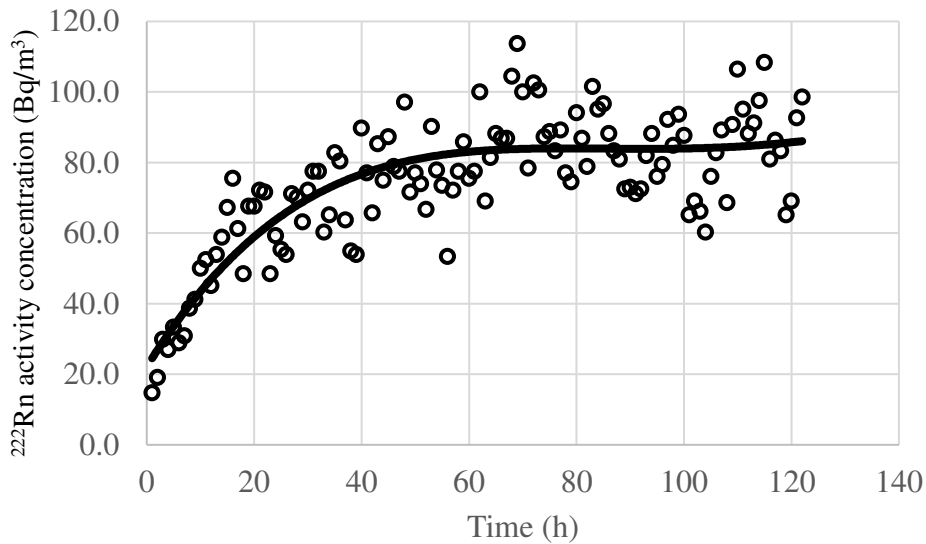


175
176 *Figure 4 - Pictures of CR39 devices (left) and the optical microscope Politrack (right)*

177

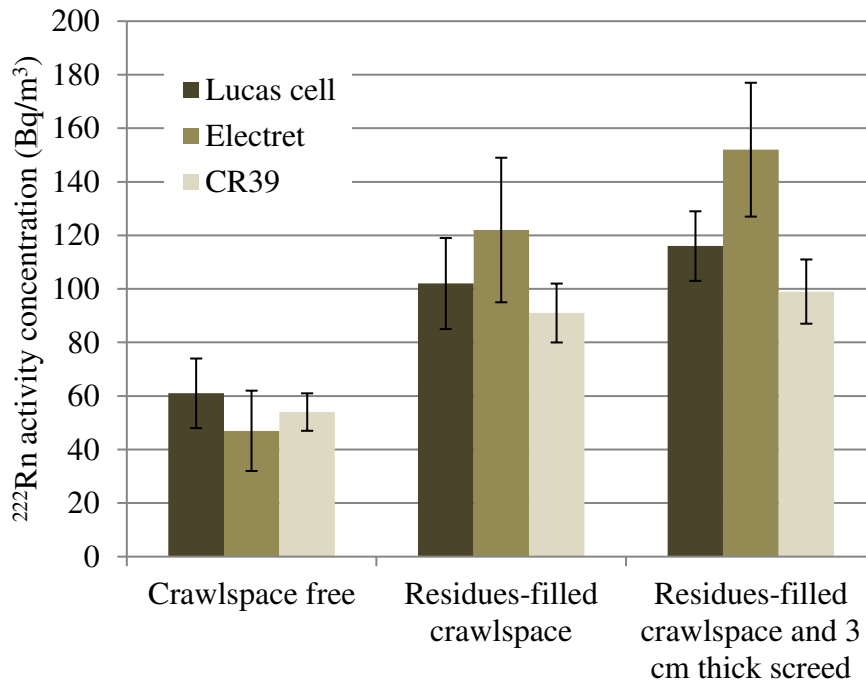
178 **5 – Results**

179 The house model was built in the central structure of Arpacal, Agency for the protection of the
180 environment of Calabria Region, in Italy, where the annual average concentration of the ^{222}Rn
181 activity is $35 \pm 12 \text{ Bq/m}^3$. However, in order to increase the accuracy of the background estimation,
182 we monitored the ^{222}Rn activity inside the model before filling the crawlspace with the phosphorite
183 residues. In Fig.5, we plot the values of $[\text{}^{222}\text{Rn}]$ measured every hour, for 5 days, by the Lucas cell.
184 In the spite of some fluctuation ascribable to environmental parameter variation, the measurements
185 show that an activity concentration plateau is reached after a couple of days (solid line in Fig.5).
186 However, the saturation value might over- or underestimate the actual activity, that can be more
187 precisely determined in long term measurements by means of passive devices. A comparison of
188 $[\text{}^{222}\text{Rn}]$ measured by Lucas Cell, electrets and CR39s is reported in Fig.6 for three different
189 configurations: crawlspace free, residues-filled crawlspace and residues-filled crawlspace covered
190 by a 3 cm thick cement screed. The values reported are averaged over 11 CR39s and 6 electrets
191 used in two different campaigns, each of which being about 3 months long.



192
193
194
195

Figure 5 - Ongoing measurement of the background ^{222}Rn activity concentration (circles). The solid line is a guide for the eye highlighting the saturation.



196

	^{222}Rn activity concentration (Bq/m ³)		
	Crawlspace free	Residues-filled crawlspace	Residues-filled crawlspace and 3 cm thick screed
Lucas cell	61±13	102±17	116±17
Electret	47±15	122±27	152±25
CR39	54±7	91±11	99±12

197
198
199
200
201

Figure 6 - Values of the ^{222}Rn activity concentration measured by Lucas Cell, Electret and CR39 in three different configurations: crawlspace free, residues-filled crawlspace and residues-filled crawlspace covered by a 3 cm thick screed.

202 6 - Discussion

203

204 The values provided by active and passive devices are rather compatible, as shown in Fig.6. They
205 all show the same trend, i.e. a significant increase of the ^{222}Rn activity concentration due to the
206 presence of metasilicates. In fact, the measured activity doubles when residues are placed inside the
207 crawlspace, growing from about 50 Bq/m^3 (just little higher than the environmental activity because
208 of concrete, bricks and mortar used (Righi 2006)) to over than 100 Bq/m^3 . An even further increase
209 is observed when the cement screed covers the residues; the electrets provide a value over than 3
210 times higher than the background one. Coherently with literature (Keller 2001), it is possible to
211 state that ^{222}Rn can diffuse inside the cement, meaning that the latter cannot actually confine the
212 gas. Naming $[^{222}\text{Rn}]_0$ the background activity, that corresponds to the crawlspace free configuration,
213 we can write:

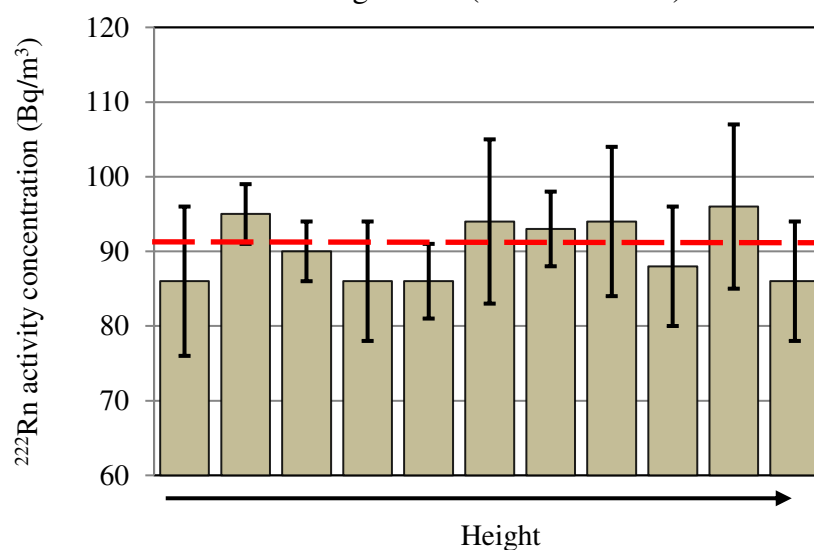
214

$$215 \quad [^{222}\text{Rn}] = [^{222}\text{Rn}]_0 + [^{222}\text{Rn}]_{\text{res}} \quad (4)$$

216

217 where $[^{222}\text{Rn}]$ is the measured value of the activity in the final configuration and $[^{222}\text{Rn}]_{\text{res}}$ is the
218 residues contribution. If we consider the most conservative situation, i.e. the highest value of the
219 activity given by the electrets, the ^{222}Rn component generated by the phosphorous materials reads
220 105 Bq/m^3 . Such a value is significantly high, being the triple of the original environmental activity.
221 One may object that even the cement screed contributes to $[^{222}\text{Rn}]_{\text{res}}$, since it might contain some
222 radionuclide. However, comparing the residues-filled crawlspace configurations with and without
223 the screed shows that the cement contribution is relatively small, and can be neglected as a first
224 approximation.

225 On the other hand, the screed presence is crucial for shielding α -, β - and γ -radiations (Han 2017).
226 By means of a radiometer, we estimated that the 3 cm thick screed is able to attenuate the γ -rays
227 generated by the phosphorous material by a factor 2. Analogously, we observed a complete
228 damping of the β contamination over the screed surface, passing from an initial value of 43 to 2 cps.
229 Finally, one may observe that the device displacement could affect the validity of the experiment.
230 This would be a non-negligible drawback in real cases, where the volume involved are much higher
231 while the number of devices remains limited. To highlight such a crucial aspect, we homogeneously
232 displaced the 11 CR39s inside the house-model and analyse the vertical distribution of the
233 measured activity, depicted in Fig.7. For sake of simplicity, we investigate in this work the sole
234 configuration of filled crawlspace without the screed. The figure clearly shows a non-monotonic
235 trend with respect to the height, clearly indicating that the ^{222}Rn activity concentration is
236 homogeneously distributed around the average value (dashed red line) in the whole volume.



237

238 *Figure 7 - Distribution of the ^{222}Rn activity concentration along the height, measured by 11 CR39s*
239 *when the crawlspace is filled with the residues before covering with the screed.*

240 **7 – Use case**

241

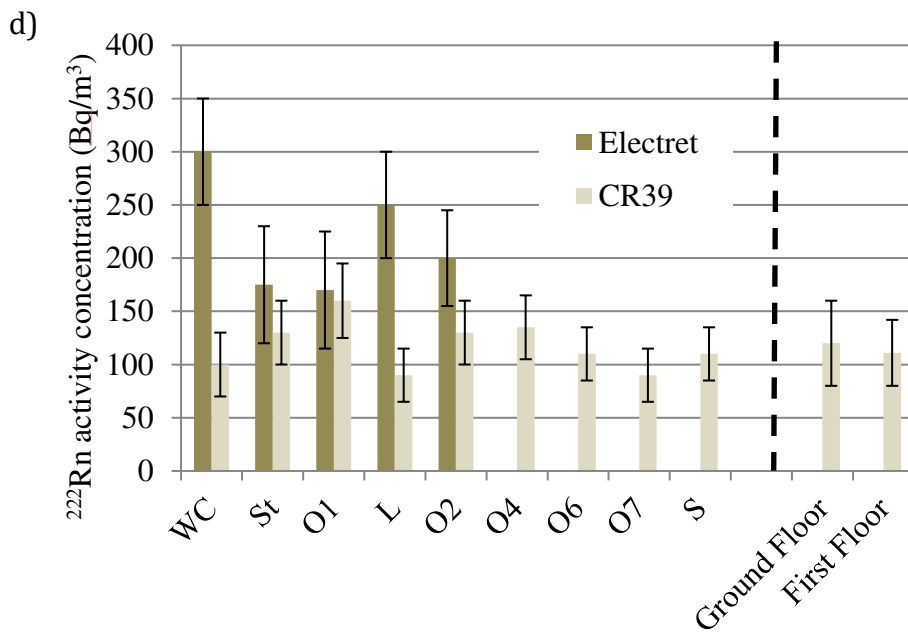
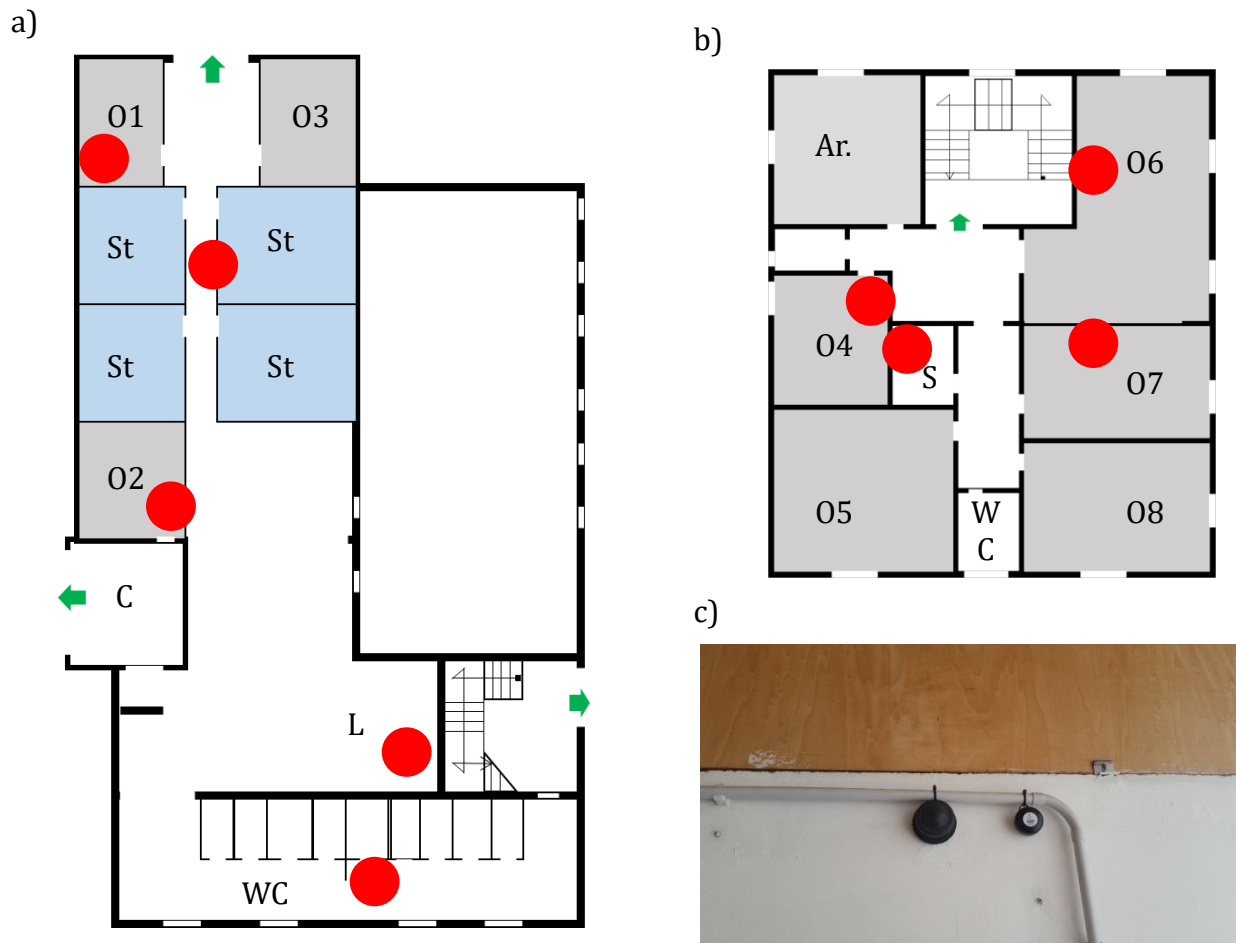
242 As a last step of our experiments, we tested the provisions given by the Mary's House model to a
243 real use case. We chose an industrial warehouse of Crotone city, located in a zone where the
244 presence of metasilicates had been previously checked. For privacy reasons, we do not provide in
245 this article details about the location of the building. However, its planimetry is sketched in
246 Fig.8a,b; the red circles stand for the exposure meter positions. We underline that the warehouse
247 was a pretty airy environment, rich of air flows, where even the heat confinement was challenging.
248 Therefore, in normal conditions, one may expect to find relatively close values of indoor and
249 outdoor [²²²Rn].

250 As for the model, we performed a 3 months long campaign. Our measurements were carried out by
251 means of 14 passive devices: 9 CR39s and 5 electrets (besides the witnesses). A picture of both the
252 devices is shown in Fig.8c while the results are reported in Fig.8d. We found a good agreement
253 between CR39 and electret measured values, that are anomalous for the territory, where the average
254 indoor [²²²Rn] ranges between 40 and 50 Bq/m³. Whereas, in our experiments values above 100
255 Bq/m³ are found, as for the Mary's house. Remarkable is the case of the WC, which was under
256 construction during the measurement campaign, and thus considerable as an outdoor environment.
257 There, we found activity values compatible with the other (indoor) rooms, meaning that there is a
258 significant contribution to the ²²²Rn activity coming from the outside. In fact, we measured a
259 remarkably high ²²²Rn activity concentration in the square facing the warehouse: active devices
260 registered values similar to the indoor experiments, while the outdoor average activity of the
261 territory is only about 15 Bq/m³. In the graph in Fig.8d, we also plot the CR39 average values of
262 each floor. One may expect to find a sharp difference between the average activity of each floor if
263 only the soil contributes to radon exhalation. Conversely, here we found almost the same activity
264 concentration values, meaning that an artificial contribution is present. This arises from
265 metasilicates inside the building structure as predicted by the model, where the [²²²Rn] vertical
266 spatial distribution is flat.

267

268

269



270
271

272
273
274
275
276
277
278
279

Figure 8 - a,b) Positioning of the CR39 in the industrial warehouse at the ground (a) and first (b) floor respectively. In the planimetry the letters stand for O (Office), St (Storage), C (Cafeteria), S (Server Room), Ar. (Archive). c) Picture of the Electret and CR39 used in the experiments. d) ^{222}Rn measured in each room and average values in each floor.

280 8 - Conclusion

281

282 We have shown how metasilicates-containing TENORM contribute to ^{222}Rn activity. A house-
283 model was realized by employing TENORM as building materials. These have a non-negligible
284 ^{238}U component, responsible of a significant increase of the ^{222}Rn activity that becomes more than
285 twice higher than the background benchmark. This result was tested by using both active and
286 passive devices, whose measurements found a rather good agreement. The spatial distribution of the
287 gas inside the house-model volume was investigated; we found an homogeneous distribution of the
288 activity with respect to the height. The model results were compared with a real use case: a
289 warehouse in the Crotone industrial zone. As predicted by the model, we found unusual values and
290 spatial distribution of the ^{222}Rn activity, indicating the presence of metasilicates inside the building
291 structure. In this sense, measuring the ^{222}Rn activity is a practical way to indirectly determine if and
292 where TENORM are employed in the construction of a building. In particular, we remark that the
293 average [^{222}Rn] measured inside the warehouse is about 120 Bq/m^3 , while the typical [^{222}Rn] values
294 of Crotone indoor environment are more than twice lower (between 40 and 50 Bq/m^3). In terms of
295 perspective, the house-model can be used to verify whether artificial ventilation can be useful to
296 significantly quench the ^{222}Rn activity concentration in a controlled environment with a known
297 volume. Our results shade a light on the employing of phosphorites factories residues that,
298 considered inert materials, were used to build roads and houses in the city, underrating the radon
299 issue. We highlight that, if controlled, a recycle of the residues is still possible. Surely, they must
300 not be used for school or warehouse building, as in our study case, but they might find application
301 in outdoor environments. Nevertheless, for these applications, particular attention must be paid to
302 water drainage, and phosphorite residues must be used only far from aquifers. Furthermore, the
303 erosive action of the sea breeze and the physiological deterioration due to atmospheric agents must
304 be considered. These may attack the silica component of the residues, producing an increase of the
305 particulate matter (mainly heavy radioactive nano- and picoparticles that maybe redeposited on the
306 surface). We conclude underlining the peculiarity of Crotone city, where a flood of the Esaro river
307 (that is dangerously close to the industrial zone, as shown in Fig.1b) may further unearth residues
308 and bring them to the sea and to the beaches, possibly producing an even greater exposition of the
309 population.

310

311 Acknowledgment

312 This study is part of the project “Mary’s House” that started in 2015 for which we would like to
313 thank S. Coppola, G.Ranieri, S. Pascuzzi and M. Bonanno for their collaboration as well as the
314 enterprise STS, Solar Technology System, for providing us the building materials. We finally
315 acknowledge the Arpacal scientific direction for the fruitful discussions.

316

317 **Author contribution** All authors contributed to the study conception and design. Material
318 preparation, data collection were performed by S.P. Analysis were carried out by A.N. and M.R.L.
319 The first draft of the manuscript was written by M.F. and all authors commented on previous
320 versions of the manuscript. All authors read and approved the final manuscript.

321

322 **Funding** This research did not receive any specific grant from funding agencies in the public,
323 commercial, or not-for-profit sectors.

324

325 **Data availability** All data generated or analysed during this study are included in this published
326 article.

327

328 Declarations

329

- **Ethics approval and consent to participate.** Not applicable.
- **Consent to publish** Not applicable.
- **Competing interests** The authors declare no conflict of interest.

330

331

332

333 **References**

334

335 Andresz S. et al., Optimization of radiation protection: Alara, a practical guidebook. 2019.

336 Bossew P., The radon emanation power of building materials, soils and rocks. Applied radiation
337 and isotopes, 59(5-6):389–392, 2003.

338 Caresana M. et al., Uncertainties evaluation for electrets based devices used in radon detection.
339 Radiation protection dosimetry, 113(1):64–69, 2005.

340 Caridi F. et al., Natural radioactivity measurement sand dosimetric evaluations in soil samples with
341 a high content of NORM. The European Physical Journal Plus, 132(1):1–6, 2017.

342 Dentoni V. et al., Natural radioactivity and radon exhalation rate of Sardinian dimension stones.
343 Construction and Building Materials, 247:118377, 2020.

344 Dimova N.T. and Burnett W.C., Evaluation of groundwater discharge into small lakes based on the
345 temporal distribution of radon-222. Limnology and Oceanography, 56(2):486–494, 2011.

346 El Afifi E.M. et al., Evaluation of U, Th, K and emanated radon in some NORM and TENORM
347 samples. Radiation Measurements, 41(5):627–633, 2006.

348 El Afifi E.M. et al., Characterization of phosphogypsum wastes associated with phosphoric acid and
349 fertilizers production. Journal of Environmental Radioactivity, 100(5):407–412, 2009.

350 Erkens W.H.H., Electro-thermal phosphorus production radioactivity in the workplace: the
351 consequences for the operators concerned in managing internal exposure (Proc. 3rd
352 European ALARA Network Workshop Neuherberg, Germany, 1999)
353 <http://www.eu-alara.net/images/stories/pdf//program3/S5Erkens.pdf>, 1999.

354 Euratom - Council directive 2013/59/euratom of 5 december 2013.

355

356 Fleischer R.L. and Mogro-Campero A., Mapping of integrated radon emanation for detection of
357 long-distance migration of gases within the earth: Techniques and principles. Journal of
358 Geophysical Research: Solid Earth, 83(B7):3539–3549, 1978.

359 Han B. et al., Radiation shielding concrete. In Smart and Multifunctional Concrete Toward
360 Sustainable Infrastructures, pages 329–337. Springer, 2017.

361 <https://eur-lex.europa.eu/legal-content/EN/TXT/PDF/?uri=CELEX:32013L0059&from=EN>.

362 Keller G. et al., Radon permeability and radon exhalation of building materials. Science of the total
363 environment, 272(1-3):85–89, 2001.

364 Kropat G. et al., Calibration of the politrack@system based on cr39 solid-state nuclear track
365 detectors for passive indoor radon concentration measurements. Radiation protection
366 dosimetry, 167(1-3):302–305, 2015.

367 Lysandrou M. et al., Radon emanation from phosphogypsum and related mineral samples in cyprus.
368 Radiation Measurements, 42(9):1583–1585, 2007.

369 Menzel R.G., Uranium, radium, and thorium content in phosphate rocks and their possible radiation
370 hazard. Journal of Agricultural and Food Chemistry, 16(2):231–234, 1968.

371 Nero A.V. and Nazaroff W.W., Characterizing the source of radon indoors. Radiation Protection
372 Dosimetry, 7(1-4):23–39, 1984.

373 Noguchi M. and Wakita H., A method for continuous measurement of radon in groundwater for
374 earthquake prediction. Journal of Geophysical Research, 82(8):1353–1357, 1977.

375 Pommé S., Solar influence on radon decay rates: irradiance or neutrinos? The European Physical
376 Journal C, 79(1):1–9, 2019.

377 Righi S. and Bruzzi L., Natural radioactivity and radon exhalation in building materials used in
378 italian dwellings. Journal of environmental radioactivity, 88(2):158–170, 2006.

379 Rutherford P.M. et al., Radon emanation coefficients for phosphogypsum. Health physics,
380 69(4):513–520, 1995.

381 Sahu P. et al., Radon emanation from low-grade uranium ore. Journal of environmental
382 radioactivity, 126:104–114, 2013.

- 383 Santagati S.M.R. et al., La concentrazione di attività di radon in un'abitazione contaminata da
384 NORM, valutazione e stima del rischio.
385 URL: https://www.soc.chim.it/sites/default/files/chimind/pdf/2016_4_42_ca.pdf. (in italian).
386 Silva P.S.C. et al., Environmental contamination by technologically enhanced naturally occurring
387 radioactive material-TENORM: A case study of phosphogypsum. *Journal of*
388 *Radioanalytical and Nuclear Chemistry*, 269(3):739–745, 2006.
- 389 Stoulos S. et al., Assessment of natural radiation exposure and radon exhalation from building
390 materials in Greece. *Journal of Environmental Radioactivity*, 69(3):225–240, 2003.
- 391 Tayibi H. et al., Environmental impact and management of phosphogypsum. *Journal of*
392 *environmental management*, 90(8):2377–2386, 2009.
- 393 Tufail M. et al., Hazard of norm from phosphorite of Pakistan. *Journal of Hazardous Materials*,
394 176(1-3):426–433, 2010.
- 395 Yanchao S. et al., Study on a new charcoal closed chamber method for measuring radon exhalation
396 rate of building materials. *Radiation Measurements*, 134:106308, 2020.
- 397 Zhang L. et al., Accurate measurement of the radon exhalation rate of building materials using the
398 closed chamber method. *Journal of Radiological Protection*, 32(3):315, 2012.

Figures

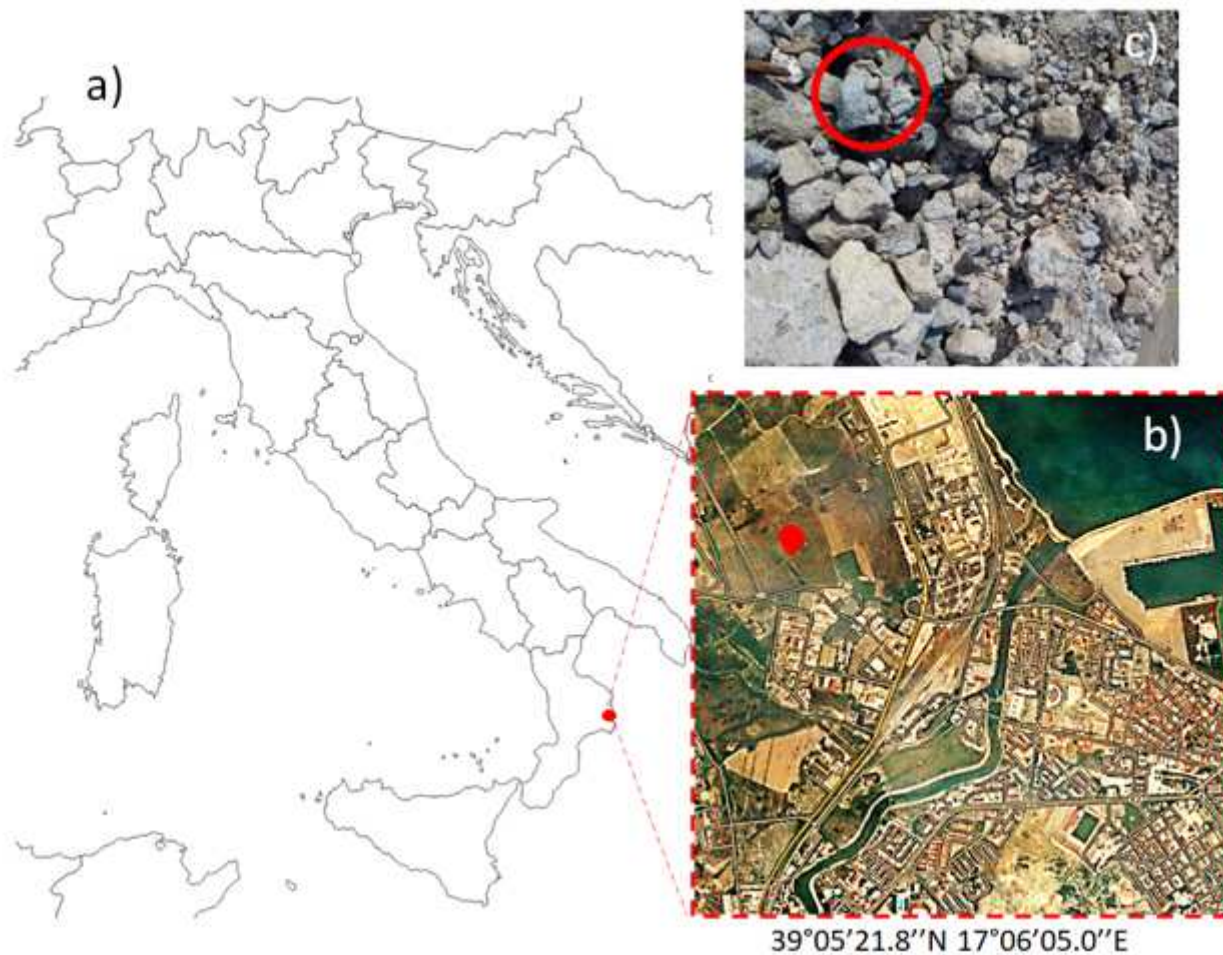
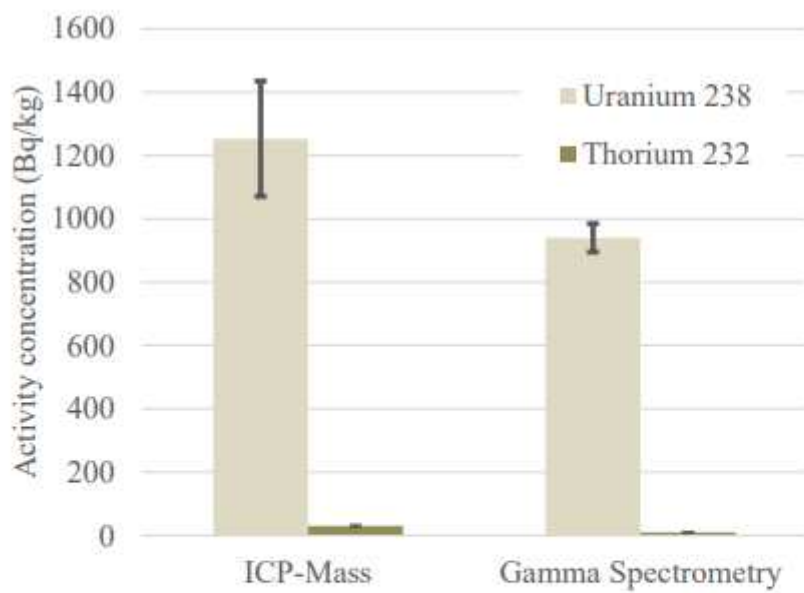


Figure 1

a) Crotona position in the Italian map. b) Harvesting site location. c) Picture of the phosphorite rocks showing their typical blue colour. Note: The designations employed and the presentation of the material on this map do not imply the expression of any opinion whatsoever on the part of Research Square concerning the legal status of any country, territory, city or area or of its authorities, or concerning the delimitation of its frontiers or boundaries. This map has been provided by the authors.



	Activity concentration [Bq/kg]	
	ICP-Mass	γ -spectrometry
²³⁸ U	1253±182	940±45
²³² Th	30±4	10±2

Figure 2

Uranium and Thorium activity concentration measured by ICP-Mass and γ -spectrometry.

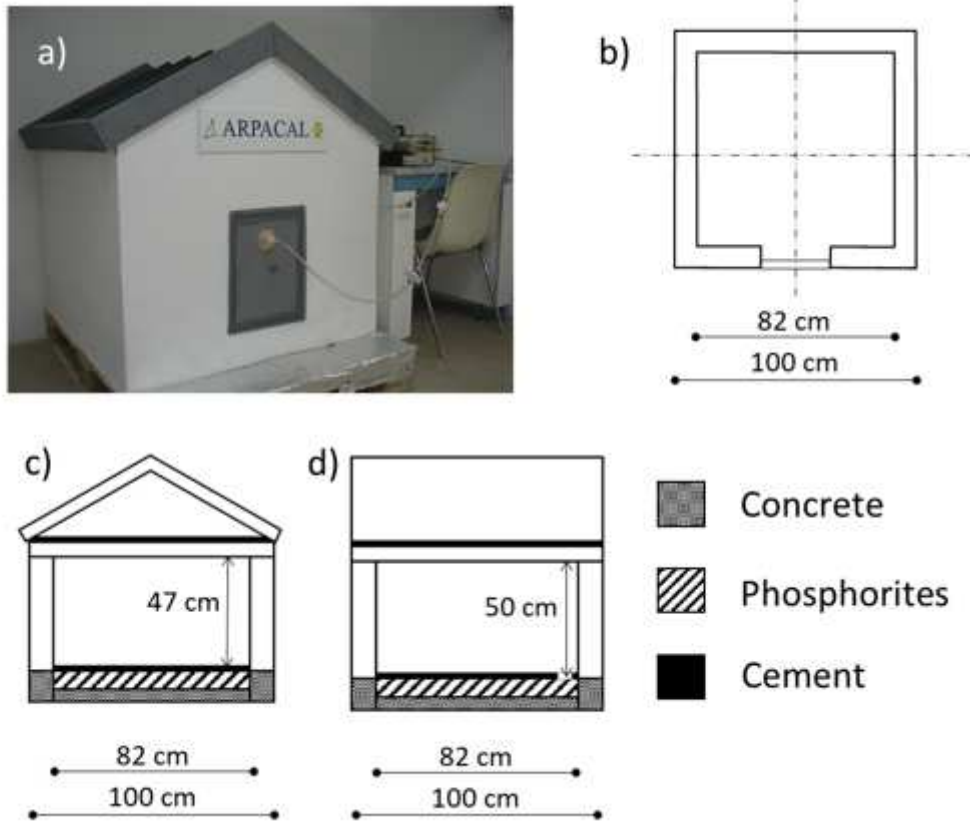


Figure 3

Building Details of Mary's House. a) Picture of the in-scale house model; b) Planimetry of the house; c-d) Model sections along the two dashed lines in b) with building material details.



Figure 4

Pictures of CR39 devices (left) and the optical microscope Politrack (right)

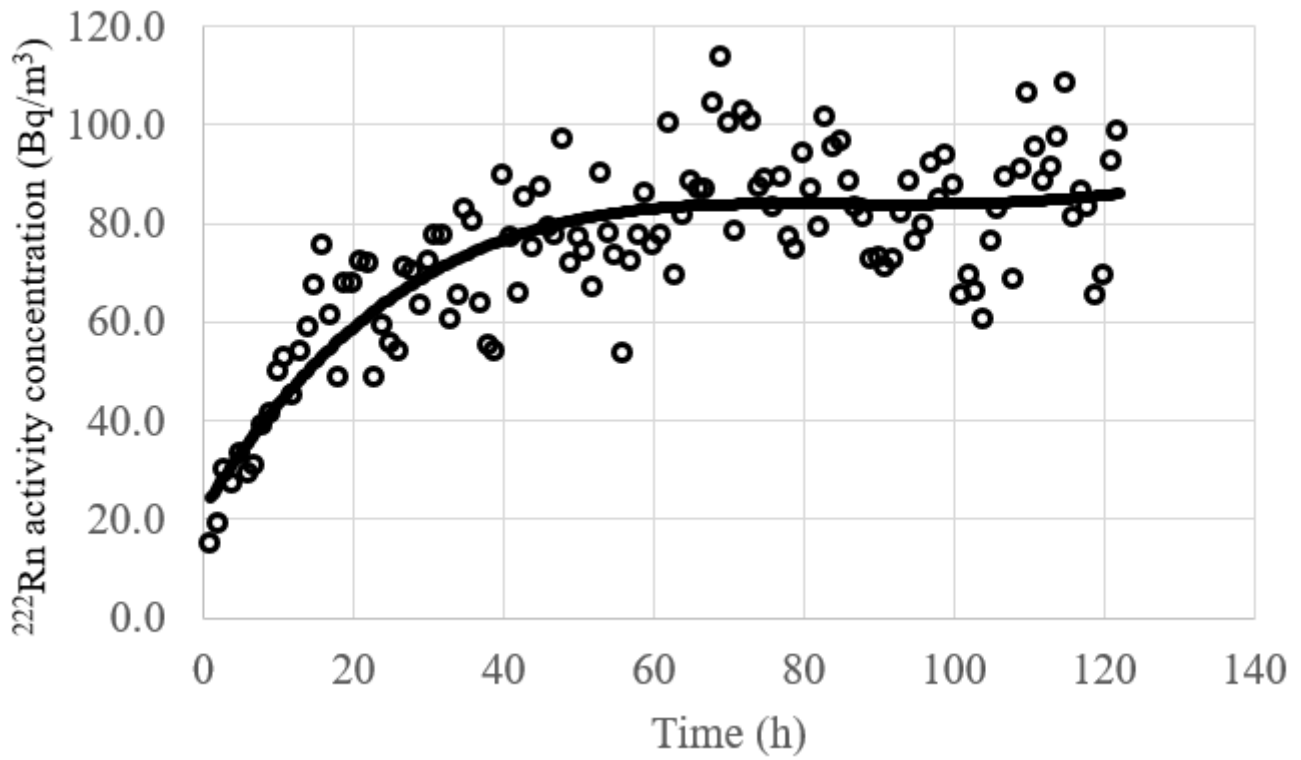
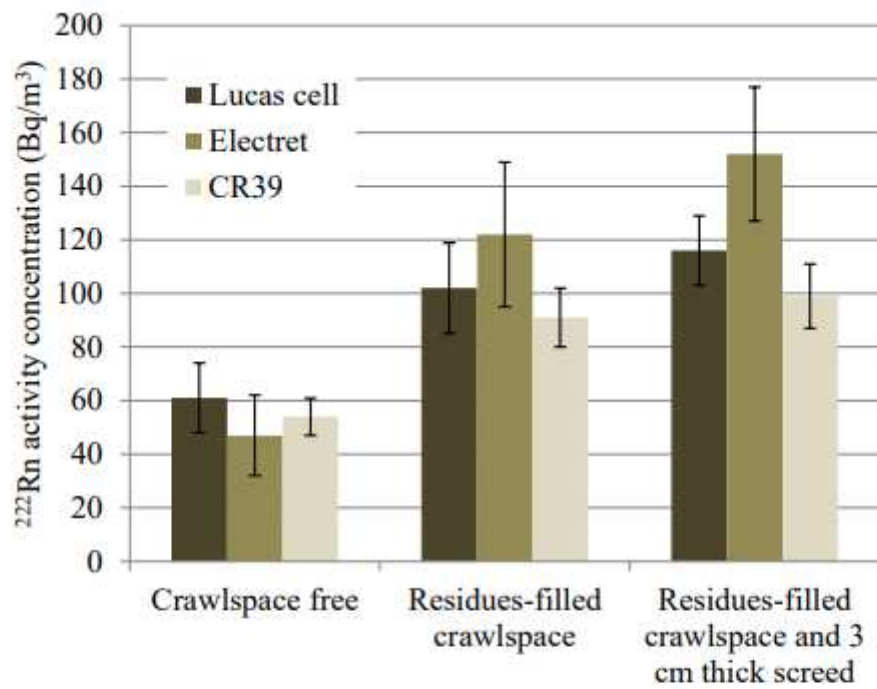


Figure 5

Ongoing measurement of the background ^{222}Rn activity concentration (circles). The solid line is a guide for the eye highlighting the saturation.



	^{222}Rn activity concentration (Bq/m^3)		
	Crawlspace free	Residues-filled crawlspace	Residues-filled crawlspace and 3 cm thick screed
Lucas cell	61±13	102±17	116±17
Electret	47±15	122±27	152±25
CR39	54±7	91±11	99±12

Figure 6

Values of the ^{222}Rn activity concentration measured by Lucas Cell, Electret and CR39 in three different configurations: crawlspace free, residues-filled crawlspace and residues-filled crawlspace covered by a 3 cm thick screed.

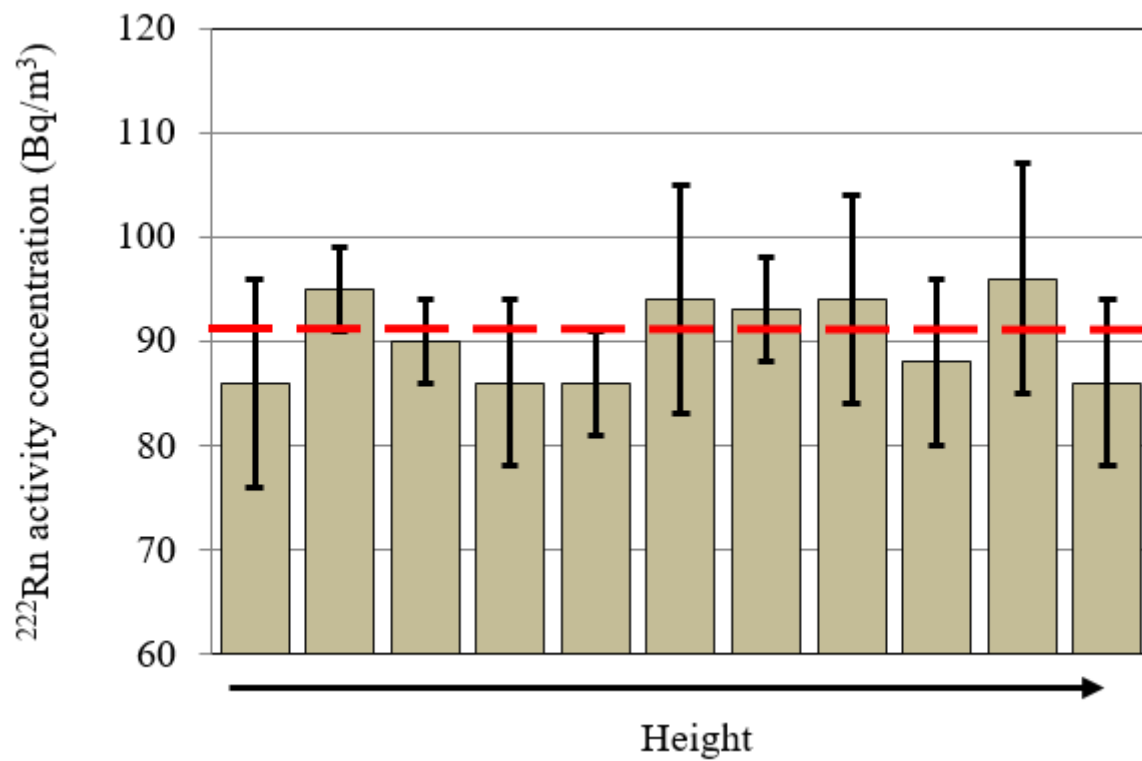


Figure 7

Distribution of the ^{222}Rn activity concentration along the height, measured by 11 CR39s when the crawlspace is filled with the residues before covering with the screed.

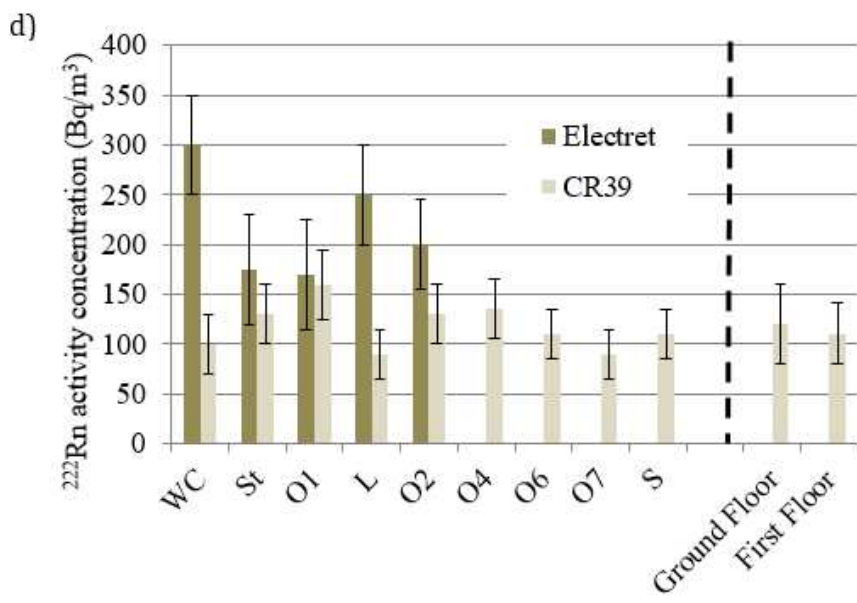
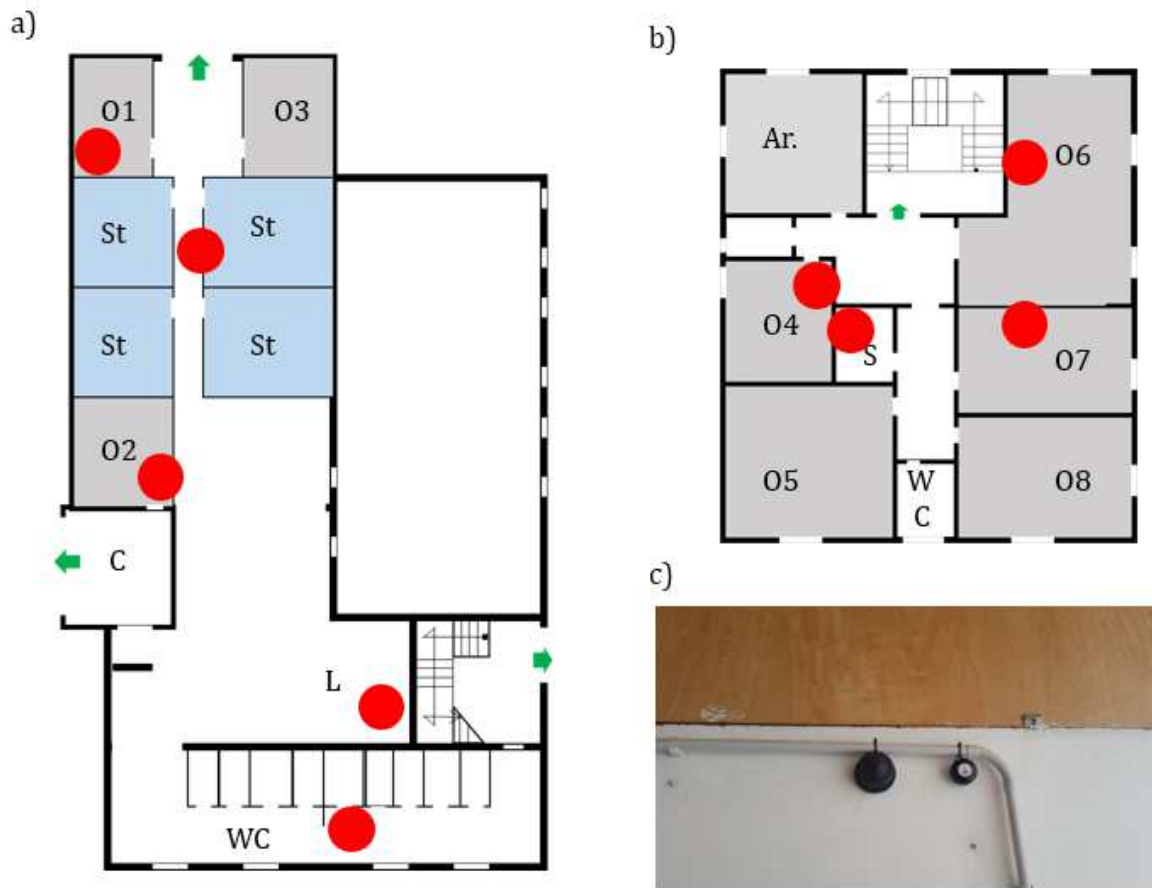


Figure 8

a,b) Positioning of the CR39 in the industrial warehouse at the ground (a) and first (b) floor respectively. In the planimetry the letters stand for O (Office), St (Storage), C (Cafeteria), S (Server Room), Ar. (Archive). c) Picture of the Electret and CR39 used in the experiments. d) [^{222}Rn] measured in each room and average values in each floor.